POSSIBLE MEASUREMENTS OF GPDs AT COMPASS

N. d'Hose[1], *E. Burtin*[1], *P.A.M. Guichon*[1], *J. Marroncle*[1], *M. Moinester*[2], *J. Pochodzalla*[3], *A. Sandacz*[4]

[1] CEA-Saclay, SPhN-DAPNIA-DSM, F-91191 Gif-sur-Yvette, Cedex, France

[2] School of Physics and Astronomy, Tel Aviv University, 69978 Ramat Aviv, Israel

[3] Johannes Gutenberg-Universität Mainz, Becherweg 45, D-55099 Mainz, Germany

[4] Soltan Institute for Nuclear Studies, ul. Hoza 69, PL-0681 Warsaw, Poland

Abstract

This paper presents the reactions which can be performed at COMPASS to study the Generalized Parton Distributions (GPDs). The high-energy muon beam at CERN allows one to measure Hard Exclusive Meson Production or Deeply Virtual Compton Scattering (DVCS) in the Bjorken regime in a large range of Q^2 and x_{Bj} ($1.5 \leq Q^2 \leq 7.5$ GeV^2 and $0.03 \leq x_{Bj} \leq 0.25$). Exploratory measurements dedicated to ρ^0 or π^0 production can be investigated with the present setup. DVCS measurement requires an upgrade of the COMPASS setup.

1. GOAL OF AN EXPERIMENT WITH THE HIGH ENERGY MUON BEAM

The Generalized Parton Distributions (GPDs) provide a unified description of the nucleon. As explained by M. Diehl [1], they interpolate between the parton distributions and the hadronic form factors. Experimentally the GPDs can be accessed in exclusive measurements such as Hard Exclusive Meson (ρ, π...) Production (HEMP) and Deeply Virtual Compton Scattering (DVCS). The latter reaction is the simplest from the theoretical point of view but also the most difficult experimentally because one has to select perfectly the final state (one lepton, one proton and one photon) among all the possible reactions. In practice we can now start the investigation of Meson Production and we foresee an upgrade of the COMPASS setup for DVCS measurement.

Experiments have already been undertaken at very high energy with the HERA collider to study mainly the gluon GPDs at very small x_{Bj} ($\leq 10^{-2}$). Larger values of x_{Bj} have been investigated in fixed target experiments at JLab (6 GeV, with plans for an upgrade at 11 GeV) and HERMES (at 27 GeV). The experimental program using COMPASS at CERN (at 100 and/or 190 GeV) will enlarge the kinematical domain to a large range of Q^2 and x_{Bj} ($1.5 \leq Q^2 \leq 7$ GeV^2 and $0.03 \leq x_{Bj} \leq 0.25$) (see Fig. 1). A large range in Q^2 is required to control the factorization in a hard, perturbatively calculable amplitude and a soft amplitude which is parametrized by the generalized parton distributions $H, E, \tilde{H}, \tilde{E}$. The GPDs depend on three kinematical variables: x and ξ parametrize the longitudinal momentum fractions of the partons, while t relates to the transverse momentum transfer.

Fig. 1: Kinematical coverage for various planned or proposed experiments. The limit $s \geq 6$ GeV^2 assures to be above the resonance domain, and $Q^2 > 1.5$ GeV^2 allows one to reach the Deep Inelastic regime.

Since the theoretical proof of factorization assumes that the transfer t is finite (that is $t/Q^2 \to 0$) [1, 2], we consider in the following $|t|$ smaller than 1 GeV^2. Another condition of factorization concerns the helicity of the virtual photon. In case of Hard Exclusive Meson Production it is mandatory
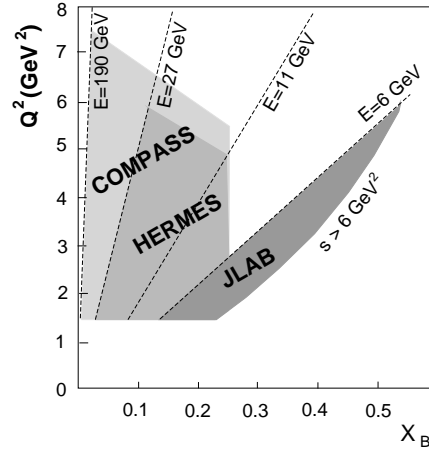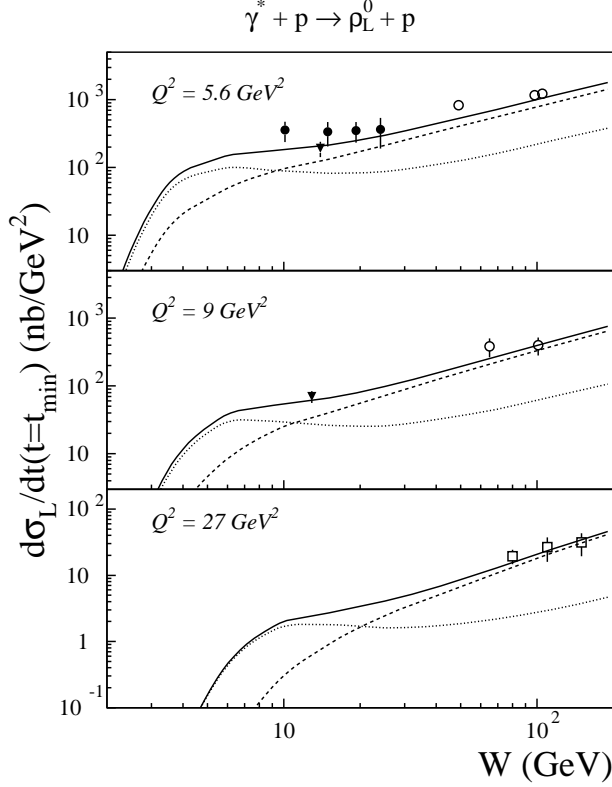
$$\gamma^* + p \rightarrow \rho_L^0 + p$$

Fig. 2: Longitudinal forward differential cross section for ρ_L^0 production (Fig. from Ref. [3]). Predictions reproduce quark contributions (dotted lines), gluon contributions (dashed lines) and the sum of both (full lines). The data are from NMC (triangles) [4], E665 (solid circles) [5], ZEUS 93 (open circles) [6] and ZEUS 95 (open squares) [7].

to impose that the virtual photon be longitudinal in order to select the perturbative gluon exchange. Experimentally we should consider Rosenbluth separation for π^0 production, while for ρ^0 production we can select longitudinal ρ^0's through the angular distribution of the decay products and assume the s-channel helicity conservation. Hard Exclusive Meson Productions seem more complex to analyse as they contain non-perturbative information on both the target and the produced meson. Nevertheless they offer the possibility to disentangle different GPDs (vector meson production depends on H and E only; pseudo-scalar production depends on $\tilde{H}$ and $\tilde{E}$ only) and to separate contributions from different flavours. Forward differential longitudinal ρ_L^0 electroproduction cross section measurements which provide the largest counting rates, have already been undertaken and are presented in Fig. 2 as a function of c.m. energy W for three values of Q^2 (5.6, 9 and 27 GeV^2). The theoretical curve is an incoherent sum of the quark and gluon contributions [3]. No measurement has been done at x_{Bj} larger than 0.05. Thanks to the expertise of the NMC Collaboration for these absolute measurements we will explore a larger domain in x_{Bj}, Q^2 and t with the muon beam available at CERN.

Deeply virtual Compton scattering is accessed by photon lepto-production: $lp \rightarrow l'p'\gamma$. In this reaction, the final photon can be emitted either by the leptons (Bethe–Heitler process) or by the proton (genuine DVCS process). If the lepton energy is large enough (see Fig. 3 with $E_\mu = 190$ GeV, $Q^2 = 4$ GeV^2, $x_{Bj} = 0.1$), the DVCS contribution dominates over the BH contribution so that the cross section is essentially the square of the DVCS amplitude which, at leading order, has the form:

$$T^{DVCS} \sim \int_{-1}^{+1} \frac{H(x,\xi,t)}{x-\xi+i\epsilon}dx\ldots \sim \mathcal{P}\int_{-1}^{+1}\frac{H(x,\xi,t)}{x-\xi}dx\ldots - i\pi H(\xi,\xi,t)\ldots$$

(where $\xi \sim x_{Bj}/2$ and t are fixed by the experiment). At smaller lepton energy (see Fig. 3 with $E_\mu = 100$ GeV and same values of Q^2 and x_{Bj} as above), the interference between BH and DVCS becomes
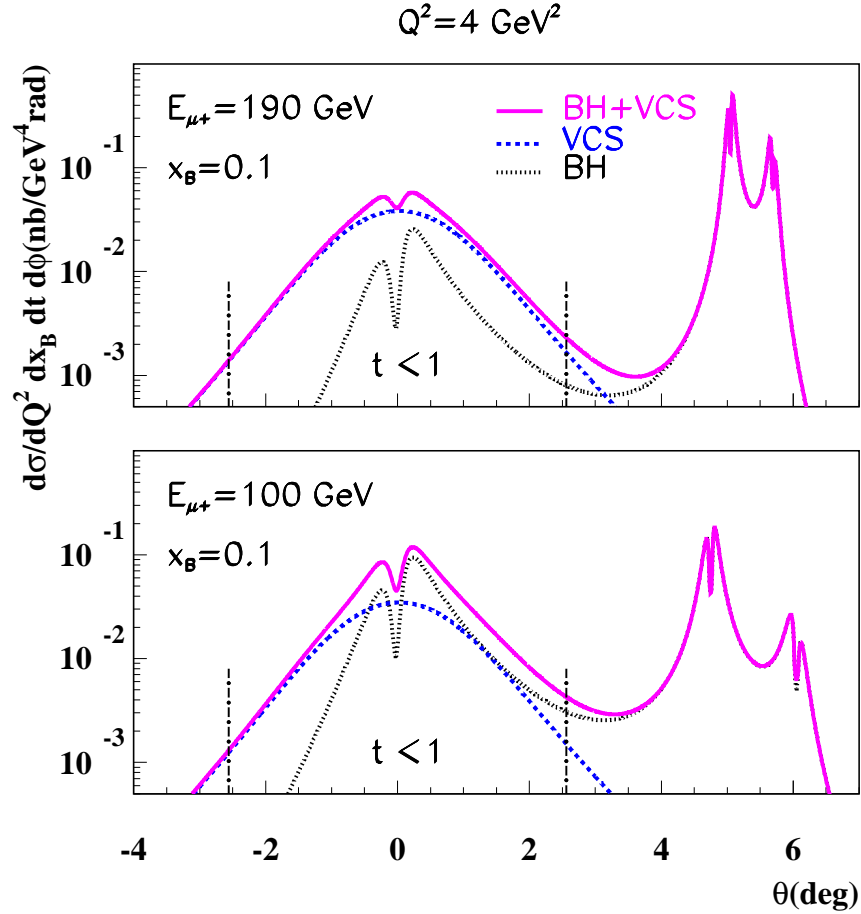
Fig. 3: Cross sections for the photon leptoproduction $\mu p \rightarrow \mu p \gamma$ as a function of the outgoing real photon angle (relative to the virtual photon direction). Comparison between BH (dotted lines), DVCS (dashed lines) and the total cross sections (full lines) for two energies of the muon beam available at CERN: 190 and 100 GeV. The interesting domain is limited by a transfer $|t|$ smaller than 1 GeV^2, i.e. θ investigating a small region around 0 degree.

large and offers a unique opportunity to study Compton scattering amplitude including its phase. A careful analysis of the dependence of the cross section on the azimuthal angle ϕ between the leptonic and hadronic planes and on Q^2 allows one to disentangle higher-twist effects and to select the real or imaginary parts of the DVCS amplitude (see the details in the previous text of M. Diehl [1]). If a longitudinally polarized lepton beam and an unpolarized target are used, the angular analysis and the Q^2 dependence of the cross section difference $\sigma(e^\uparrow) - \sigma(e^\downarrow)$ allow one to select the imaginary part of the DVCS amplitude and thus the GPDs at the specific values $x = \xi$. This study is being investigated at HERMES [8] and JLab [9]. If two muon beams of opposite charge and polarization are used, the angular analysis and the Q^2 dependence of the sum of cross sections $\sigma(\mu^{+\downarrow}) + \sigma(\mu^{-\uparrow})$ allow also one to select the imaginary part of the DVCS amplitude. Moreover the same method applied to the difference of cross sections $\sigma(\mu^{+\downarrow}) - \sigma(\mu^{-\uparrow})$ allows one to select the real part of the DVCS amplitude which, for a given ξ, is sensitive to the complete dependence on x of the GPDs. The deconvolution (over x) of this formula to extract the GPDs is not yet clearly solved, but comparison to model predictions can easily be made. It is clear that the muon beam of high energy at CERN can offer many possibilities in order to investigate the many-faceted problem of the GPDs knowledge.

Figure 4 shows the azimuthal distribution of the charge asymmetry which can be measured at COMPASS and the strong sensitivity to two different models [10]. The first one is based on a simple parametrization of the GPDs: $H^f(x, \xi, t) = H^f(x, \xi, 0) F_1^f(t)/2$ where $F_1^f(t)$ represents the elastic
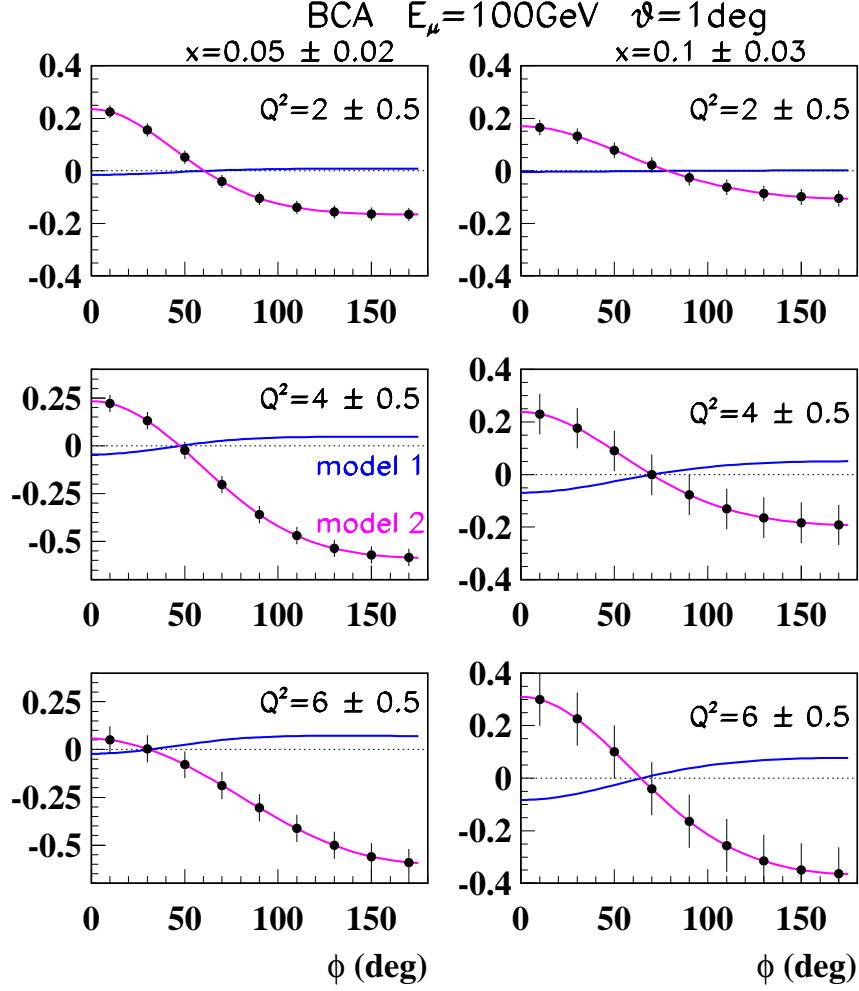
Fig. 4: Azimuthal distribution of the beam charge asymmetry measured at COMPASS at $E_\mu = 100$ GeV and $|t| \leq 0.6$ GeV^2 for two domains of x_{Bj} ($x_{Bj} = 0.05 \pm 0.02$ and $x_{Bj} = 0.10 \pm 0.03$) and three domains of Q^2 ($Q^2 = 2 \pm 0.5$ GeV^2, $Q^2 = 4 \pm 0.5$ GeV^2 and $Q^2 = 6 \pm 0.5$ GeV^2) obtained in six months of data taking with a global efficiency of 25% and with $2 \cdot 10^8$ μ per SPS spill ($P_{\mu^+} = -0.8$ and $P_{\mu^-} = +0.8$).

Dirac form factor for the quark flavour f in the nucleon. The second one [11–14] relies on the fact that the GPDs measure the contribution of quarks with longitudinal momentum fraction x to the corresponding form factor as is suggested by the sum rule:

$$\int_{-1}^{+1} H^f(x, \xi, t)dx = F_1^f(t).$$

As one can associate the Fourier transform of form factors with charge distributions in position space, one can expect that the GPDs contain information about the distribution of partons in transverse position space. In fact it has been demonstrated that, when t is purely transverse which amounts to $\xi = 0$, then $H(x, 0, t)$ is the Fourier transform of the probability density to find a quark with momentum fraction x at a given distance from the centre of momentum in the transverse plane. Qualitatively one expects that quarks with a large x come essentially from the small valence 'core' of the nucleon, while the small x region should receive contributions from the much wider meson 'cloud'. Therefore one expects a gradual increase of the t-dependence of $H(x, 0, t)$ as one goes from larger to smaller values of x. This suggests the parametrization: $H(x, 0, t) = q(x)e^{t\langle b_\perp^2 \rangle} = q(x)/x^{\alpha t}$ where $\langle b_\perp^2 \rangle = \alpha \cdot \ln \frac{1}{x}$ represents the increase of the nucleon transverse size with energy. The domain of small x_{Bj} reached at COMPASS is related to

the observation of see quarks or meson 'cloud' or also gluons and it provides a large sensitivity to this three-dimensional picture of partons inside a hadron.

2. GENERAL REQUIREMENTS FOR COMPASS

The highest luminosity reachable at COMPASS is required to investigate these exclusive measurements. The experiment will use 100–190 GeV/c muons from the M2 beam line. Limits on radio-protection in the experimental hall imply that the maximum flux of muon to be expected is of $2 \cdot 10^8$ muons per SPS spill (5.2 s spill duration, repetition each 16.8 s). Under these circumstances, we can reach a luminosity of $\mathcal{L} = 5 \cdot 10^{32}$ cm^{-2}s^{-1} with the present polarized ^{6}LiD or NH$_3$ target of 1.2 m long, and only a luminosity of $\mathcal{L} = 1.3 \cdot 10^{32}$ cm^{-2}s^{-1} with a future liquid hydrogen target of 2.5 m length.

In order to get useful cross sections with positive and negative muon beams, it is necessary to perform a precise absolute luminosity measurement. This has already been achieved by the NMC Collaboration within a 1% accuracy [15]. The integrated muon flux was measured continuously by two methods: either by sampling the beam with a random trigger (provided by the α emitter ^{241}Am) or by sampling the counts recorded in two scintillator hodoscope planes used to determine incident beam tracks. The beam tracks were recorded off-line, in the same way as the scattered muon tracks, to determine exactly the integrated usable muon flux.

Moreover μ^+ and μ^- beams of 100 GeV energy, with the same and as large as possible intensity as well as exactly opposite polarization (to a few %) are required. The muons are provided by pion and kaon decay and are naturally polarized. The pions and kaons come from the collision of the SPS 400 GeV proton beam on a Be primary target. A solution was proposed by Lau Gatignon [16]. It consists in: 1) selecting 110 GeV pion beams from the collision and 100 GeV muon beams after the decay section in order to maximize the muon flux; 2) keeping constant the collimator settings which define the pion and muon momentum spreads (both the collimator settings in the hadron decay section and the scrapper settings in the muon cleaning section) in order to fix the μ^+ and μ^- polarizations at exactly the opposite value ($P_{\mu^+} = -0.8$ and $P_{\mu^-} = +0.8$); 3) fixing N_{μ^-} to $2 \cdot 10^8$ μ per SPS spill with the longest 500 mm Be primary target; 4) using a shorter target to find N_{μ^+} close to $2 \cdot 10^8$ μ per SPS spill.

This paragraph presents the experimental procedure to select the exclusive HEMP or DVCS channel and the difference equipments that are required. They are mostly part of the existing high-resolution COMPASS spectrometer: muon detection which insures a good resolution in x_{Bj} and Q^2, meson detection and identification in RICH or photon detection in calorimeters of good energy and position resolutions to allow two-photon separation. The COMPASS spectrometer intercepts only forward outgoing particles (until 10 degrees) and the photon or meson detection limits the experiment to small x_{Bj} values ($x_{Bj} \leq 0.15$). At these high energies the complete final state, including the low-energy recoiling proton, needs to be detected because missing-mass techniques are not efficient due to the experimental resolutions (the resolution in missing mass which is required is $(m_p + m_\pi)^2 - m_p^2 = 0.25$ GeV^2 and the experimental resolution which can be achieved is larger than 1 GeV^2). Consequently the high-resolution COMPASS spectrometer needs to be completed by a recoil detector to measure precisely the proton momentum and exclude other reactions under high-luminosity conditions. In the next section we shall try to by-pass the necessity of a recoil detector to investigate the cleanest channel: $\mu p \to \mu p \rho^0$ where ρ^0's are identified through their decay to two charged pions accurately measured in the forward COMPASS spectrometer.

3. A PRAGMATIC SOLUTION WITH THE PRESENT SETUP

With the present COMPASS setup we can undertake Hard Exclusive ρ^0 Production (with the largest cross section) as we can benefit from the good expertise for this measurement in the previous NMC and SMC experiments and so produce data in this field as soon as possible. At the same time we can also investigate Hard Exclusive π^0 Production to see the limit of this setup.

In this context the constraints and limits of these experiments are the following:

1) With the present polarized ^{6}LiD or NH$_3$ target the production occurs on quasi-free nucleons in the nucleus or in the coherent scattering on the nucleus.

2) Luminosity determination is needed, but can be realized indirectly by measuring at the same time unpolarized Deep Inelastic Scattering and using known or calculated structure functions F_2 and R (the 'EMC' nuclear effects have to be taken into account).

3) The selection of longitudinal ρ^0 will be made by the angular distribution of the decay product. No Rosenbluth separation is envisagable for π^0 production.

4) The absence of a recoil detector prevents the complete exclusivity of the channel.

Precise simulations of exclusive ρ^0 and π^0 production have been performed [17, 18] and were already presented at the COMPASS meeting in Munich in 2000. The selection of exclusive events can be summarized as follows:

1) Deep inelastic events are selected by cuts on variables depending on the scattered muon kinematics:
$$2 \leq Q^2 \leq Q^2_{max} \text{ and } 35(20) \leq \nu \leq 170(90) \text{ GeV for } \rho^0$$
$$1 \leq Q^2 \leq Q^2_{max} \text{ and } 15(10) \leq \nu \leq 170(85) \text{ GeV for } \pi^0$$
The values outside(inside) the brackets correspond to the beam energy of 190(100) GeV.

2) ρ^0 and π^0 are identified through decays: $\rho^0 \rightarrow \pi^+\pi^-$ and $\pi^0 \rightarrow \gamma\gamma$. Only two hadrons of opposite charge associated with the vertex defined by the incident and scattered muons are required for ρ^0 production and only two photons with the incident and scattered muons are demanded for π^0 production. For ρ^0, hadrons have to be identified as pions. It is then required that each pion decay is emitted in the laboratory at an angle smaller than 180 mrad (the acceptance limit of the forward spectrometer) and its momentum is above 2 GeV. For π^0 it is demanded that each decay photon has energy above 2 GeV and enters either electromagnetic calorimeter ECAL1 or ECAL2. In addition, the separation of two photons at the entrance of a calorimeter should be larger than 4 cm.

3) To isolate at best the exclusive ρ^0 events, a cut on the inelasticity I [1] is used. In Fig. 5 the inelasticity distribution is shown for the SMC ρ^0 sample [19] for the events with the invariant mass in the central part of the ρ^0 invariant mass peak. For the inelasticity distribution the peak at $I = 0$ is the signal of exclusive ρ^0 production. Non-exclusive events, where in addition to detected fast hadrons, slow undetected hadrons are produced, appear at $I \geq 0$. However, due to the finite resolution, they are not resolved from the exclusive ρ^0 peak. For the cut $-0.05 \leq I \leq 0.05$ defining the exclusive sample, the amount of the residual non-exclusive background for the SMC experiment was up to about 10% at large Q^2.

4) Finally for the ρ^0 channel a cut on the invariant mass of the two pions can be applied in order to reduce the non-resonant background. For the SMC sample the invariant mass distribution after selections, including the cut on inelasticity, is shown in Fig. 5. Although the shape of the mass spectrum varies with Q^2, a mass cut, i.e. $0.62 \leq m_{\pi^+\pi^-} \leq 0.92$ GeV^2, allows a selection of ρ^0 events with the relatively low amount of non-resonant background.

It is clear that the good resolution on charged particles associated to ρ^0 decay allows the criteria 3 and 4 and thus provides a good signature of the exclusive ρ^0 channel. The selection of the π^0 channel depends strongly on the quality of the electromagnetic calorimeters, but constraints cannot be so nicely determined.

The simulation uses event generators based on a traditional parametrization on NMC data for ρ^0 production and on two models of GPDs for π^0 production. Secondary interactions of the decay charged pions, absorption of the decay photons in the target, kinematical smearing based on the experimental resolution, trigger acceptance, acceptance for pions and photons and track reconstruction efficiency are considered. A global ρ^0 selection efficiency which takes into account secondary interactions, three-track efficiency, two-pion acceptance, a cut on I and $M_{\pi^+\pi^-}$ and muon trigger acceptance is evaluated to

---

[1] $I = \frac{M_X^2 - M_p^2}{W^2}$ where $W^2 = (p + q)^2$ is the total energy squared in the virtual photon–proton system and $M_{X^2} = (p + q - v)^2$ is the missing mass squared of the undetected recoiling system (p, q, v are the four-momenta of the target proton, virtual photon and meson respectively.)
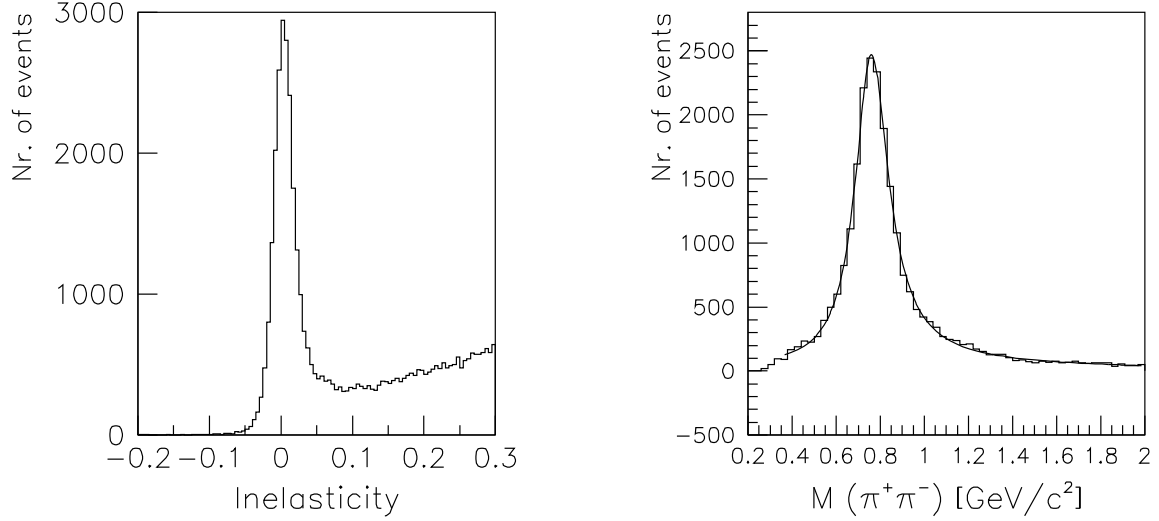
Fig. 5: The SMC results [19] for $\mu N \rightarrow \mu \rho^0 N$. (left) Inelasticity distribution after selections; (right) mass spectrum after selection including the cut $-0.05 \leq I \leq 0.05$. The full line represents a prediction according to the Söding model.

Table 1: Total cross sections and counting rates.

	190 GeV	100 GeV	
$\sigma^{tot}_{\mu N \rightarrow \mu X}$	48 nb	38 nb	
$\sigma^{tot}_{\mu N \rightarrow \mu \rho^0 N}$	286 pb	250 pb	$\langle Q^2 \rangle \sim 2.9$
$N^{cuts}_{\mu N \rightarrow \mu \rho^0 N}/year$	97 kevents	15 kevents	$\langle x_{Bj} \rangle \sim 0.034$
$\sigma^{tot}_{\mu N \rightarrow \mu \pi^0 N}$	1.3 to 5.2 pb	5.8 to 23 pb	$\langle Q^2 \rangle \sim 1.6$
$N^{cuts}_{\mu N \rightarrow \mu \rho^0 N}/year$	625 to 2500 events	1860 to 7440 events	$\langle x_{Bj} \rangle \sim 0.040$

0.21(0.04) with the medium Q^2 trigger (which consists of the 'middle trigger' and the 'ladder trigger' of the muon trigger hodoscopes) and to 0.36(0.30) with the full Q^2 range trigger (which includes, in addition, the newly implemented 'outer trigger'). The values outside(inside) the brackets correspond to the beam energy of 190(100) GeV. A global π^0 selection efficiency which takes into account secondary interaction, two-photon acceptance and muon-trigger acceptance is found close to 0.30.

Total cross sections integrated over the Q^2 and ν acceptance and expected counting rates (with the medium Q^2 trigger) for a period of 150 days (1 year) assuming an overall SPS and COMPASS efficiency of 25% are presented in Table 1. The two limits for π^0 production correspond to the two models. About two-thirds of the produced ρ^0 are longitudinally polarized.

The background to the reaction $\mu N \rightarrow \mu \rho^0 N$ has been studied. It is due to the events with at least two slow undetected particles which are outside the acceptance of the spectrometer or for which tracks are not reconstructed due to inefficiency and which pass all selections for exclusive ρ^0 events. A first possible source of this background is ρ^0 production with diffractive dissociation of the target $\mu N \rightarrow \mu \rho^0 N^*$ with the subsequent decay of the excited state N^* in $N + k\pi$. In the lower part of Fig. 6 a schematic drawing of the inelasticity distribution for these events is presented. Although the smearing effects are not taken into account it is clear that the events from diffractive dissociation of the target into the lowest masses excitations of the nucleon will contribute to the exclusive ρ^0 sample in the inelasticity cut. An estimation has been found close to 20%.

A second source of background will originate from the large number of inclusive deep inelastic events. Simulation with a sample of 5000 events only, using the generators LEPTO and JETSET, has given an
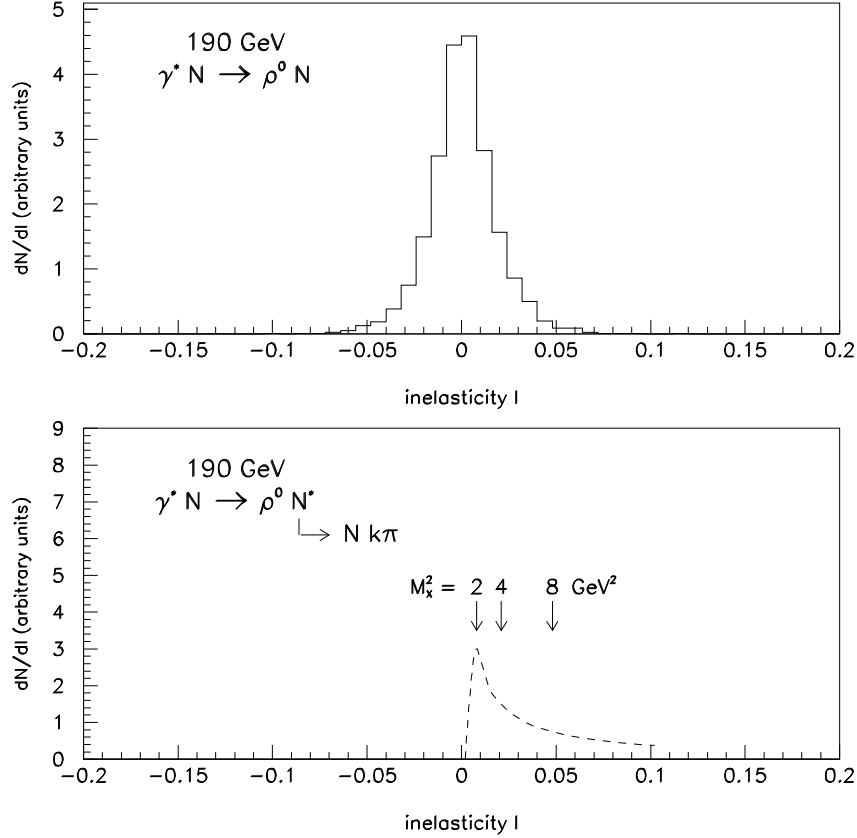
Fig. 6: Inelasticity distribution for the simulated $\mu N \rightarrow \mu \rho^0 N$ events at 190 GeV; (bottom) calculated distribution of the inelasticity for $\mu N \rightarrow \mu \rho^0 N^*$ for a continuum distribution of N^* masses.

upper limit of contamination of 20% also.

4. AN IDEAL SOLUTION WITH A COMPLETED SETUP

As mentioned in the previous section it is clear that only a recoil detector which allows low-energy recoiling proton detection will help to select exclusive channels such as HEMP or DVCS. The latter reaction is surely the most delicate because one has to select a final state with one muon, one photon and one low-energy proton among many competing reactions listed below:

1) Hard Exclusive π^0 Production $\mu p \rightarrow \mu p \pi^0$ where π^0 decays in two photons, for which the photon with higher energy imitates a DVCS photon, and the photon with smaller energy is emitted at large angle outside of the acceptance or its energy is below the photon detection threshold.

2) Diffractive dissociation of the proton $\mu p \rightarrow \mu \gamma N^*$ with the subsequent decay of the excited state N^* in $N + k\pi$. (The low-energy pions are emitted rather isotropically.)

3) Inclusive Deep Inelastic Scattering with, in addition to the reconstructed photon, other particles produced outside the acceptance or for which tracks are not reconstructed due to inefficiency.

Moreover one has to take into account a background which includes beam halo tracks with hadronic contamination, beam pile-up, particles from the secondary interactions, and external bremsstrahlung.

A simulation has been realized in order to define the proper geometry of the detector complementing the present COMPASS setup and to analyse the operational conditions. The goal was to maximize the ratio of DVCS events over DIS events for a sample of events with one muon and one photon in the COMPASS spectrometer acceptance plus only one proton of momentum smaller than 750 MeV/c and angle larger than 40 degrees (it is the typical kinematics of a DVCS event at small t). The simulation relies on the event generator program PYTHIA 6.1 [20] which includes most of the known processes [21]
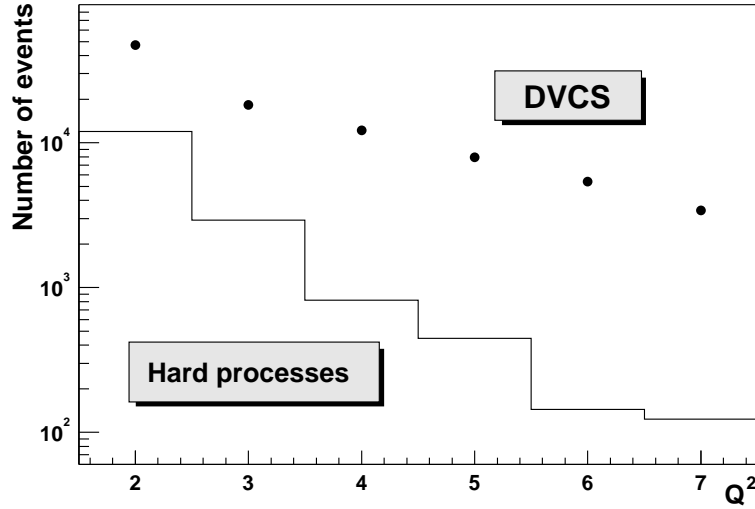
Fig. 7: Number of events for DVCS (dots) and DIS (histogram) processes as a function of Q^2 for selection of events with only one muon, one photon and one recoiling proton and condition for charged particle detection up to 40 degrees and for photon detection up to an angle of 24 degrees and above a threshold of 50 MeV.

such as Deeply Inelastic Scattering and Deeply Meson Production. The experimental parameters such as maximum angle and energy threshold for photon detection and maximum angle for charged particle detection could then be tuned. With photon detection extended up to 24 degrees and above an energy threshold of 50 MeV and with charged particle detection up to 40 degrees, one observes that the number of DVCS events as estimated with models is more than an order of magnitude larger than the number of DIS events over the whole useful Q^2 range (see Fig. 7).

The COMPASS setup will be instrumented with two electromagnetic calorimeters ECAL1 and ECAL2 [22, 23]. They are mainly constituted of lead-glass blocks called GAMS. They are cells of 38.4 × 38.4 × 450 mm^3. Typical characteristics of such calorimeter are:

- energy resolution: $\sigma P_\gamma / P_\gamma = 0.055/\sqrt{P_\gamma} + 0.015$,
- position resolution: $\sigma_x = 6.0/\sqrt{P_\gamma} + 0.5$ in mm,
- high rate capability: 90% of signal within 50 ns gate with no dead time,
- effective light yield: about 1 photoelectron per MeV; hence low-energy photons of down 20 MeV can be reconstructed.

The separation of the overlapping electromagnetic showers in the cellular GAMS calorimeter is carefully studied in Ref. [24]. The result of the study shows that at 10 GeV one can reach a 100% level of the separation efficiency for a minimum distance between two photon tracks at the entrance of the calorimeter of $D = 4$ cm. The last value is slightly shifted to $D = 5$ cm at 40 GeV.

This excellent performance of the calorimeters will provide a key role in the perfect separation between DVCS events and hard π^0 events.

One possible solution to complement the present COMPASS setup is presented in Fig. 8. It consists of one recoil detector described below, an extended calorimetry from 10 to 24 degrees, and a veto for charged forward particles until 40 degrees. This calorimeter has to work in a crowded environment and in a magnetic fringe field of SM1 and therefore it has to be studied further.

At the present time our studies have focused on the possibility to design and successfully operate a dedicated recoil detector. One goal is to identify and measure the protons' momenta between a minimum value and 750 MeV/c. A solution consists in a large time-of-flight setup between a thin segmented cylindrical layer of scintillator counters, about 3m long and surrounding the 2.5 m long target, and a
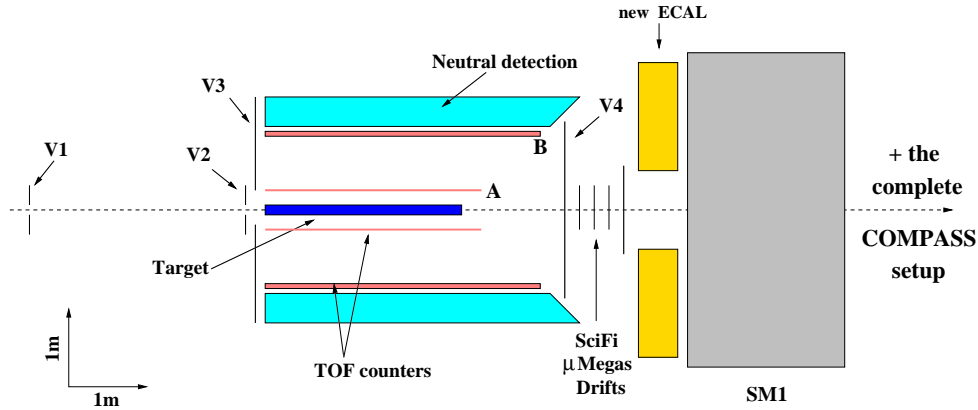
Fig. 8: Proposal for a detector complementing the COMPASS setup. A recoil detector, an extended calorimetry from 10 to 24 degrees, and a veto (V4) for charged forward particles until 40 degrees have been added.

thick layer at about 1 m distance from the first layer. The thickness of the first layer has to be as small as possible in order to detect protons of minimum momentum. With an hydrogen target of 3 cm diameter, target wall thickness of about 3 mm of equivalent scintillator and a first layer of 4 mm, a minimum momentum of 270 MeV/c is reached. All the counters are read at both sides by photomultiplier counters to determine time and position with very accurate resolutions (300 ps and 1.8 cm). The consequent resolution in momentum varies from 3 to 10%. The resolution in t is twice this value, thus it is very desirable to further study all the parameters which can be improved. Moreover, the exclusion of extra particles has to be studied with kinematical fits depending on the experimental resolution and/or with low-energy π^0 detection. This detector has to work in a high-rate environment. It has to be as large and hermetic as possible within a reasonable cost. The actual realisation of such performances is under active investigation.

Counting rates, given in Table 2, have been estimated assuming six months of data taking (1 year) assuming an overall efficiency of 25% and considering the present COMPASS setup where the photon detection is limited to 10 degrees plus a proton detection from 250 to 750 MeV/c ($|t| \leq 0.64$ GeV^2). This statistics allows for the ϕ distribution presented in Fig. 4 for $Q^2 = 2$, 4 and 6 GeV^2 and $x_{Bj} = 0.05$ and 0.10. Studies devoted to the t dependence of the cross section can be investigated but for that it is quite worth while to try to improve the t resolution.

We have tested the concept of this detector using the already existing muon beam and a simplified setup (one sector of scintillators with reduced length). The muon beam was scattered off a 10 cm long polyethylene target, mostly equivalent in radiation length to the foreseen long liquid hydrogen target. We used three scintillators read out at both sides, a 4 mm thick one close to the target (A), a 5 cm thick one 80 cm away from the target (B) and an extra scintillator (C) to know if particles go through B or are stopped in B. The rates observed in the scintillator close to the target, using the nominal intensity of $2 \cdot 10^8$ muons per spill, is of the order of 1 MHz (mainly due to Möller electrons). It demonstrates that the background environment is acceptable for the time-of-flight system.

The result of the time of flight operation [see Fig. 9(a)] shows a clear proton signal. With the knowledge of the β velocity and the energy lost in B for stopped particles, one can reconstruct their masses. It is done in Fig. 9(b) where one can see pions, protons and deuterons for raw data, corrected data and the target out contribution which is about two orders of magnitude smaller.

The position resolution obtained on A and B and the time-of-flight resolution are better than 2 cm and 300 ps respectively. Extension to long (3 m) and thin scintillators have to be studied carefully and technology has to be improved to achieve still better resolution. An efficiency study of such a recoil detector is being performed.

Table 2: Number of events for bins in x_{Bj} and Q^2.

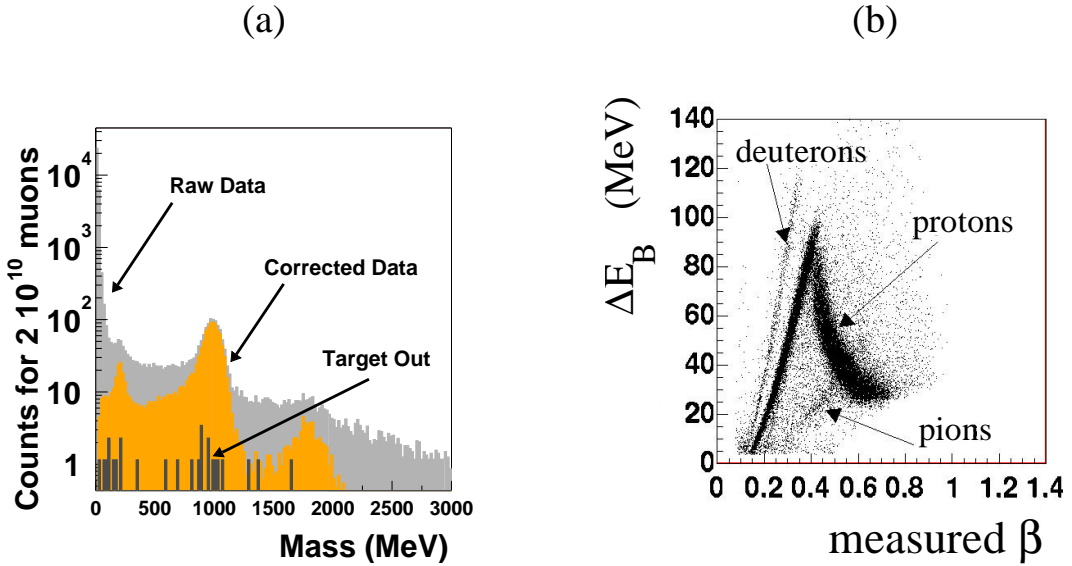| $E_\mu = 190$ GeV			
	$x_{Bj} = 0.05 \pm 0.02$	$x_{Bj} = 0.10 \pm 0.03$	$x_{Bj} = 0.20 \pm 0.07$
$Q^2 = 2 \pm 0.5$	10058	8897	2000
$Q^2 = 3 \pm 0.5$	3860	2540	1300
$Q^2 = 4 \pm 0.5$	2058	1136	600
$Q^2 = 5 \pm 0.5$	1472	677	520
$Q^2 = 6 \pm 0.5$	875	459	357
$Q^2 = 7 \pm 0.5$	642	299	242
$E_\mu = 100$ GeV			
	$x_{Bj} = 0.05 \pm 0.02$	$x_{Bj} = 0.10 \pm 0.03$	$x_{Bj} = 0.20 \pm 0.07$
$Q^2 = 2 \pm 0.5$	13670	9921	4300
$Q^2 = 3 \pm 0.5$	5933	3200	2000
$Q^2 = 4 \pm 0.5$	4532	1537	770
$Q^2 = 5 \pm 0.5$	3000	995	600
$Q^2 = 6 \pm 0.5$	1806	885	499
$Q^2 = 7 \pm 0.5$	810	870	352

(a) (b)

Fig. 9: (a): Energy lost in the B scintillator as a function of the measured β. (b): Mass distribution of particles stopped in B. The three peaks are pions, protons and deuterons respectively.

5. CONCLUSIONS

This study takes advantage of the high energy of the muon beam available at CERN which provides a large Q^2 and x_{Bj} range and encourages us for the following roadmap. Hard Exclusive Meson Production has to be undertaken as soon as possible with the present setup. A large number of ρ^0 events (a few 10K) can be produced in one year. The ρ^0 channel which decays in $\pi^+\pi^-$ is the easiest channel to isolate, the π^0 channel is more difficult but very important to test the calorimetry performances. A complete experiment with both Hard Exclusive Meson Production with a large set of mesons and Deeply Virtual Compton Scattering has to be envisaged in a next step with a completed COMPASS setup. For this purpose one needs a 'long' hydrogen target, a recoil detector, and an extension of the calorimetry at larger angles.

COMPASS is the unique place which provides μ^+ and μ^- of 100 GeV in order to study carefully two scales of observation $x_{Bj} = 0.05 \pm 0.02$ and $x_{Bj} = 0.10 \pm 0.03$ on a large domain of Q^2 from 2 to 7 GeV^2 and to measure the azimuthal distribution of the Beam Charge Asymmetry which seems very promising to test the geometrical interpretation of GPDs.

Acknowledgements

References

[1] M. Diehl, Introduction to Generalized Parton Distributions, Contribution to these Proceedings.

[2] J.C. Collins, L. Frankfurt and M. Strikman, Phys. Rev. D **56** (1997) 2982.

[3] M. Vanderhaeghen, P.A.M. Guichon and M. Guidal, Phys. Rev. **D 60** (1999) 094017.

[4] NMC Collaboration, M. Arneodo *et al.*, Nucl. Phys. B **429** (1994) 503.

[5] E665 Collaboration, M.R. Adams *et al.*, Z. Phys. C **C74** (1997) 237.

[6] ZEUS Collaboration, M. Derrick *et al.*, Phys. Lett. B **356** (1995) 601.

[7] ZEUS Collaboration, J. Breitweg *et al.*, Eur. Phys. J. C **6** (1999) 603.

[8] HERMES Collaboration, A. Airapetian *et al.*, Phys. Rev. Lett. **88** (2001) 182001.

[9] CLAS Collaboration, S. Stepanyan *et al.*, Phys. Rev. Lett. **87** (2001) 182002.

[10] L. Mossé, P.A.M. Guichon and M. Vanderhaeghen, private communication.

[11] M. Burkardt, Phys. Rev. D **62** (2000) 07503; hep-ph/0207047.

[12] J.P. Ralston and B. Pire, hep-hp/0110075.

[13] M. Diehl, Eur. Phys. J. C **25** (2002) 233; ibid. C **31** (2003) 277 (E).

[14] A.V. Belitsky and D. Müller, Nucl. Phys. A **711** (2002) 118; hep-hp/0206306.

[15] NMC Collaboration, P. Amaudruz *et al.*, Phys. Lett. B **295** (1992) 159; R.P. Mount, Nucl. Instrum. Meth. **187** (1981) 401.

[16] L. Gatignon, private communication.

[17] J. Pochodzalla, L. Mankiewicz, M. Moinester, G. Piller, A. Sandacz and M. Vanderhaeghen, hep-ex/9909534.

[18] A. Sandacz, COMPASS Note 2000-1 (2000).

[19] A. Tripet, presented at the 7th International Workshop on DIS and QCD, Nucl. Phys. B , Proc. Suppl. **79** (1999).

[20] PYTHIA 6.1, User's manual, T. Sjöstrand *et al.*, High Energy Physics Event Generation with PYTHIA 6.1, Comput. Phys. Commun. **135** (2001) 238; hep-ph/0010017.

[21] C. Friberg and T. Sjöstrand, hep-ph/0007314.

[22] A Proposal for a Common Muon and Proton apparatus for Structure and Spectroscopy, CERN/SPSLC 96-14 and wwwcompass.cern.ch.

[23] V. Poliakov, Presentation of ECAL1 and ECAL2, January 25, 2001.

[24] A.A. Lednev, Separation of the overlapping electromagnetic showers in the cellular GAMs-type calorimeters, Preprint IHEP 93-153 (1993), Protvino, Russia.